

# Dissipative cooling towards phantom Bethe states in boundary driven XXZ spin chain

Vladislav Popkov<sup>1,2</sup> and Mario Salerno<sup>3</sup>

<sup>1</sup>*Faculty of Mathematics and Physics, University of Ljubljana, Jadranska 19, SI-1000 Ljubljana, Slovenia*

<sup>2</sup>*Bergisches Universität Wuppertal, Gauss Str. 20, D-42097 Wuppertal, Germany*

<sup>3</sup>*Dipartimento di Fisica “E.R. Caianiello”, and INFN - Gruppo Collegato di Salerno, Università di Salerno, Via Giovanni Paolo II, 84084 Fisciano (SA), Italy*

(Dated: June 15, 2022)

A dissipative method that allows to access family of phantom Bethe-states (PBS) of boundary driven XXZ spin chains, is introduced. The method consists in coupling the ends of the open spin chain to suitable dissipative magnetic baths to force the edge spins to satisfy specific boundary conditions necessary for the PBS existence. Cumulative monotonous depopulation of the non-chiral components of the density matrix with growing dissipation amplitude is analogous to the depopulation of high-energy states in response to thermal cooling. Compared to generic states, PBS have strong chirality, nontrivial topology and carry high spin currents.

**Introduction** Dissipation needs not to be always destructive for quantum protocols but it can represent a resource for manipulating quantum systems. Dissipation alone [1] or in combination with coherent dynamics [2–10], indeed, can be used to create quantum non-equilibrium stationary states (NESS) which are attractors of the dynamics and therefore are stable even in the presence of noise.

Most protocols, however, require a tailored set of operations used in pumping cycles to target each specific state [5, 11]. If the protocols are implemented by stationary control fields, they usually require sophisticated dissipations that make the NESS targeting more complicated [12]. This is due to the fact that the targeted NESS must be an eigenstate of the coherent part of the dynamics and a dark state for all jump operators in the dissipator [13, 14].

Here we demonstrate how to generate a remarkable family of NESS containing arbitrary number of qubits, employing simple boundary-localized dissipation, and manipulating just one parameter. These are the phantom Bethe states (PBS), i.e. eigenstates of integrable XXZ spin chains on special parameter manifolds [15–17], possessing unusual chiral and topological features.

The phenomenon is based on a subtle mechanism rendering a highly selective “phantom” invariant subspace the basin of attraction for the density matrix, in quantum Zeno limit [18–21]. As a result, the NESS responds in a singular resonant manner to an increase of dissipative strength at vicinity of “phantom” manifolds, restricting the density matrix to states with chirality of the same sign and rendering the NESS chiral. The resonances become sharper as the dissipation strength is increased and their number grows with the number of spins involved.

Dynamically, the “freezing out” of the non-chiral components of the density matrix with growing dissipation amplitude is analogous to the depopulation of high-energy states in response to thermal cooling. Thus we refer to our scenario as “dissipative cooling”.

A change of the control parameter, e.g. the misfit  $az-$

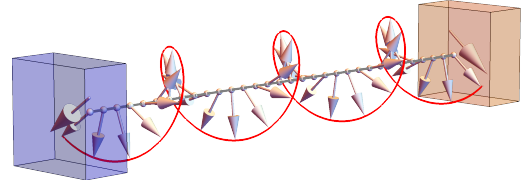


FIG. 1. Targeting a pure spin-helix state (12) of the XXZ open spin chain by coupling the boundary spins to fully polarizing baths represented by two boxes. Z axis is directed along the chain while the spin rotation occurs in XY plane perpendicular to the chain.

imuthal angle of dissipatively-targeted boundary polarizations, allows to thread “phantom” manifolds with different topology, passing from one chiral NESS to another. The stability of dissipatively created PBS is guaranteed as long as the boundary dissipation strength is kept sufficiently high. In comparison to generic pure and mixed states of the open XXZ chain, PBS have strong chirality and carry high spin currents, as demonstrated below.

**Model setting and near Zeno limit relaxation.** Our dissipative setup is schematically depicted in Fig. 1. An XXZ Heisenberg spin  $\frac{1}{2}$  chain of  $N+2$  sites, numbered as  $0, 1, \dots, N+1$ , is coupled to Lindbladian baths of polarizations at the ends ([18, 22], see details in [23]). We assume dissipative targeting of generic pure qubit states  $\rho_{L,R} = (I + \vec{n}_{L,R} \cdot \vec{\sigma})/2$  at sites 0 and  $N+1$ , where  $\vec{n}_L, \vec{n}_R$  are unit vectors of polarization. The strength of the dissipation  $\Gamma$  is measured by the inverse time needed for edge spins to relax, e.g.  $\rho_{L/R}(t) = \frac{I}{2} + \frac{1}{2}\vec{\sigma}_1\vec{n}_{L/R} + O(e^{-\Gamma t})$ , if the coherent part (XXZ spin chain Hamiltonian) is neglected. If  $\vec{n}_L \neq \vec{n}_R$ , a nonequilibrium gradient is created and a spin current  $j^z$  can flow, typically obeying the Fourier law  $j^z = O(1/N)$ . In (8) we fix a resonance condition under which steady currents can be increased up to maximally possible values,  $j^z = O(1)$ . Using criterium [24] one finds that the NESS is always unique.

It was shown in [25] that close to quantum Zeno limit  $\Gamma \rightarrow \infty$  the relaxation to NESS undergoes a three-stage

process, each stage occurring at different timescale. On the shortest timescale:  $t \leq O(1/\Gamma)$ , the boundary spins relax towards their targeted states. From this point on, the density matrix is approximately given by  $\rho = \rho_L \otimes R(t) \otimes \rho_R$ , where  $R(t) = \text{tr}_{L,R} \rho(t)$  describes the time evolution of the internal part of the system, governed by the dissipation projected Hamiltonian  $h_D$  [2] given by [25]

$$h_D = \sum_{n=1}^{N-1} \vec{\sigma}_n \cdot \hat{J} \vec{\sigma}_{n+1} + \hat{J} \vec{n}_L \cdot \vec{\sigma}_1 + \hat{J} \vec{n}_R \cdot \vec{\sigma}_N, \quad (1)$$

with  $\hat{J} = \text{diag}(1, 1, \Delta)$ . Note that dissipation-projected Hamiltonian (1) depends on polarizations of the baths through its boundary fields. On the intermediate timescale:  $O(1/\Gamma) \ll t \leq O(1)$ , the reduced density matrix  $R(t)$  acquires the approximate form

$$R(t) = \sum_{\alpha} P_{\alpha}(\tau) |\alpha\rangle\langle\alpha| + O\left(\frac{1}{\Gamma}\right), \quad (2)$$

where  $\tau = \frac{t}{\Gamma}$  and  $|\alpha\rangle$  are  $h_D$  eigenstates, with positive coefficients  $P_{\alpha}$  significantly changing on scales  $\tau = O(1)$ . Finally, on the longest time scale  $O(1) \ll t \leq O(\Gamma)$  the coefficients  $P_{\alpha}(\tau) \rightarrow P_{\alpha}(\infty) \equiv P_{\alpha}$  relax to their stationary NESS values, by following an effective Markov process

$$\frac{\partial P_{\alpha}(\tau)}{\partial \tau} = \sum_{\beta \neq \alpha} w_{\beta\alpha} P_{\beta}(\tau) - \sum_{\beta \neq \alpha} w_{\alpha\beta} P_{\alpha}(\tau) \quad (3)$$

with rates  $w_{\alpha\beta} \equiv w_{\alpha \rightarrow \beta}$  given by [25]

$$w_{\alpha\beta} = |\langle \beta | g_L | \alpha \rangle|^2 + |\langle \beta | g_R | \alpha \rangle|^2, \quad (4)$$

where  $g_L, g_R$  are operators acting on the first and the last spin respectively, given by

$$g_L = g(\vec{n}_L) \otimes I^{\otimes N-1}, \quad g_R = I^{\otimes N-1} \otimes g(\vec{n}_R), \quad (5)$$

$$g(\vec{n}(\theta, \varphi)) = \hat{J} \left( \vec{n}\left(\frac{\pi}{2} - \theta, \varphi + \pi\right) - i\vec{n}\left(\frac{\pi}{2}, \varphi + \frac{\pi}{2}\right) \right) \cdot \vec{\sigma}, \quad (6)$$

where  $\theta, \varphi$  are spherical coordinates of a unit vector. The final state, the NESS, in the Zeno limit has the form

$$\rho_{NESS}^{Zeno} = \rho_L \otimes \left( \sum_{\alpha} P_{\alpha} |\alpha\rangle\langle\alpha| \right) \otimes \rho_R, \quad (7)$$

where  $P_{\alpha}$  is time-independent solution of (3), and  $|\alpha\rangle$  are eigenstates of  $h_D$  (1).

**Phantom Bethe states.** Phantom Bethe states are eigenstates of the Hamiltonian (1) that correspond to special manifolds of the boundary fields in (1)  $\hat{J} \vec{n}_L(\theta_L, \varphi_L), \hat{J} \vec{n}_R(\theta_R, \varphi_R)$ , with  $\theta, \varphi$  given by [15, 16]

$$\theta_L = \theta_R, \quad \varphi_R - \varphi_L = (N + 1 - 2M_+) \gamma, \quad (8)$$

where  $M_+ = 0, 1, \dots, N + 1$  [26] and  $\gamma$  parametrizing the  $XXZ$  model anisotropy  $\Delta$

$$\Delta = \cos \gamma. \quad (9)$$

The substitution  $M_+ \rightarrow M_- \equiv N + 1 - M_+$  in (8) leads to the physical setup with the opposite boundary gradient,  $\varphi_R - \varphi_L \rightarrow -(\varphi_R - \varphi_L)$ , and consequently flips the steady current  $j^z \rightarrow -j^z$ . The respective NESSs are related via the left-right reflection  $\varphi_L \leftrightarrow \varphi_R$  and subsequent rotation in  $XY$ -plane, see [23]. Using this property we restrict the  $M_+$  range to the  $M_+ = 0, 1, \dots, \lfloor \frac{N+1}{2} \rfloor$ .

For fixed  $M \equiv M_+$  in this range all eigenstates  $|\alpha\rangle$  of  $h_D$  (1) which determine Zeno NESS (7) split into two chiral families,  $\{|\alpha_+\rangle\}, \{|\alpha_-\rangle\}$  characterized by the so-called phantom Bethe roots [15]. All eigenstates from each family share common chiral properties [16]. Introducing function  $b(n, m) = \sum_{k=n}^m \binom{N}{k}$ , the number of eigenstates  $d_+, d_-$  in  $\{|\alpha_+\rangle\}, \{|\alpha_-\rangle\}$  is given by  $d_{\pm} = b(0, M_{\pm})$ . Moreover, in our case (8) a smaller invariant subfamily  $\{|\alpha_+^{(1)}\rangle\} \in \{|\alpha_+\rangle\}$  exists [23], yielding further splitting  $\{|\alpha_+\rangle\} = \{|\alpha_+^{(1)}\rangle\} \oplus \{|\alpha_+^{(2)}\rangle\}$  where  $d_+^{(1)} = b(M - 1, M) = \binom{N+1}{M}$ ,  $d_+^{(2)} = b(0, M - 2)$ .

According to the above, the reduced density matrix  $R$  in (2) on “phantom” manifolds (8) splits as

$$R \approx \sum_{\kappa=1}^2 \sum_{\alpha_+^{(\kappa)}=1}^{d_+^{(\kappa)}} P_{\alpha_+^{(\kappa)}}(\tau) |\alpha_+^{(\kappa)}\rangle\langle\alpha_+^{(\kappa)}| + \sum_{\alpha_-=1}^{d_-} P_{\alpha_-}(\tau) |\alpha_-\rangle\langle\alpha_-|. \quad (10)$$

Sum (10) contains projectors on states with opposite chiralities and is generically approximately neutral. The time evolution obeys (3) i.e. depends on rates  $w_{\beta\delta}$  exclusively. Analyzing the rates [23] we find a remarkable property: all rates  $w_{\alpha_+^{(1)} \rightarrow \alpha_-} = w_{\alpha_+^{(1)} \rightarrow \alpha_+^{(2)}} = 0$  vanish, while generic  $w_{\beta \rightarrow \alpha_+^{(1)}}$  remain finite. Thus, subfamily  $\{|\alpha_+^{(1)}\rangle\}$  becomes an adsorbing basin of the Markov process (3) [27] resulting in depopulation of all other states with time, and leading to the NESS of the form

$$\rho_{NESS}^{Phantom}(M) = \rho_L \otimes \left( \sum_{\alpha_+^{(1)}=1}^{\binom{N+1}{M}} P_{\alpha_+^{(1)}} |\alpha_+^{(1)}\rangle\langle\alpha_+^{(1)}| \right) \otimes \rho_R. \quad (11)$$

All eigenstates  $|\alpha_+^{(1)}\rangle$  in (11) are phantom Bethe eigenstates [15] of the same chirality and the chirality gets more pronounced for small  $M$ . For  $M = 0$ , the sum in (11) contains one eigenfunction, which is the spin-helix state (SHS) (12),

$$\Psi_{SHS}(\gamma) = \bigotimes_{k=1}^N \begin{pmatrix} \cos \frac{\theta_L}{2} \\ \sin \frac{\theta_L}{2} e^{ik\gamma + i\varphi_L} \end{pmatrix}. \quad (12)$$

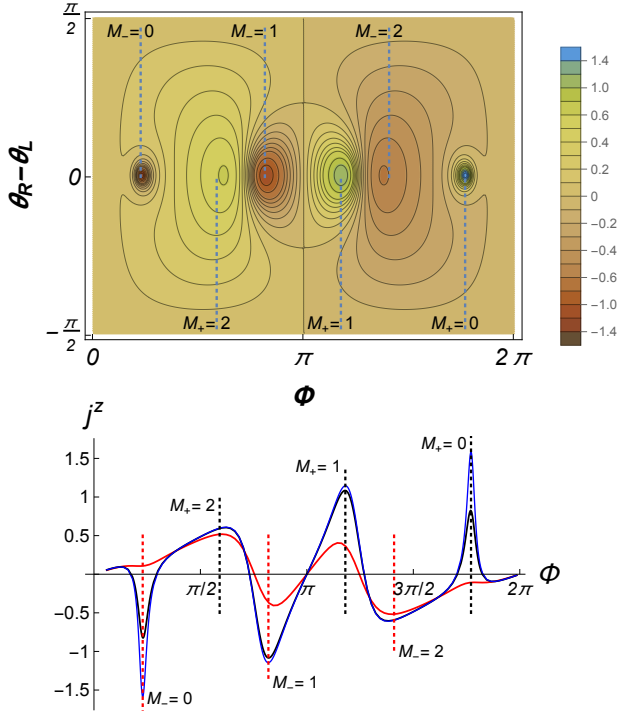


FIG. 2. **Top Panel:** Steady magnetization current  $j^z$  versus boundary gradient misfit of azimuthal angle  $\Phi = \varphi_R - \varphi_L$  and polar angle  $\theta_R - \theta_L$ , in Zeno limit, for  $N = 5, \Delta = 0.6, \theta_L = \pi/2$ . The targeted spin polarizations are  $\vec{n}_L = (1, 0, 0), \vec{n}_R = (\sin \theta_R \cos \Phi, \sin \theta_R \sin \Phi, \cos \theta_R)$ . **Bottom Panel:** cut of the  $j^z$  surface at  $\theta_R - \theta_L = 0$ , for different dissipation strengths  $\Gamma = 20, 100, 1000$  (more spiky functions correspond to increasing  $\Gamma$ ). Vertical black and red dotted lines indicate the misfit angles  $\Phi = \pm(N + 1 - 2M)\gamma$ .

visualized in Fig. 1, characterized by a large current of magnetization

$$j_{SHS} = \langle 2(\sigma_n^x \sigma_{n+1}^y - \sigma_n^y \sigma_{n+1}^x) \rangle_{SHS} = 2 \sin^2 \theta_L \sin \gamma. \quad (13)$$

A possibility to target spin-helix state (12) dissipatively was also noted in previous studies [14, 28, 29].

For  $M > 0$  ideal helix (12) gets blurred but the NESS (11) remains chiral. For  $M = 1$  the current of magnetization  $\langle \alpha_+ | \hat{j}^z | \alpha_+ \rangle$  averaged over states  $|\alpha_+ \rangle$  is of the order  $\langle j^z(M) \rangle \approx j_{SHS}(1 - 2/N)$ , while for arbitrary  $M < N/2$ , estimates yield  $\langle j^z(M) \rangle \approx j_{SHS}(1 - 2M/N)$  [16].

From the above result we predict the existence of chiral Zeno NESS with unusually high magnetization current at phantom Bethe manifolds (8).

**Numerical results.** To check our predictions we study NESS magnetization current for fixed anisotropy  $\Delta$  and varying boundary gradient, for systems of size  $4 \leq N \leq 30$ . We use exact numerical diagonalization for small chains and Matrix product ansatz for NESS in Zeno limit [30, 31] for large chains. Already for  $N = 5$  we find all  $j^z$  peaks positions at predicted points (8) and their vicinity,

see Figs. 2. Namely, all points (8) with  $M_{\pm} = 0, 1, 2$  correspond to peaks of various amplitudes ( $j^z = 0$  for  $M_{\pm} = 3$ , because it leads to zero gradient  $\vec{n}_L = \vec{n}_R$ ).

For larger chains (Fig. 3) the agreement and the phenomenon becomes striking: most  $j^z$  peaks appear as sharp resonances centered at phantom Bethe states manifolds (8), on top of a background with  $j^z = O(1/N)$ .

The role of parameter  $M$  determining the NESS rank in (11) via  $r(M) = \binom{N+1}{M}$  deserves special discussion. The highest and sharpest of all  $j^z$  peaks always corresponds to  $M_{\pm} = 0$ , see Figs. 2, 3, i.e. pure Zeno NESS, with magnetization winding in perfect helix around  $Z$  axis, see (12) and Fig. 4. For  $M > 0$ , perfect chirality is lost: the basis of “phantom” manifold for  $M = 1$  consists of 2 disjointed helix pieces separated by a kink at some position  $n$ ; phantom Bethe states are linear combinations of basis states for all possible kink positions [16]. Resulting NESS magnetization profile is a distorted helix with variable radius, see mid-panel of Fig. 4. Basis states for arbitrary  $M$  contain  $M$  kinks [16], introducing more helix imperfections. For large  $M$  NESS becomes a mixture of exponentially large number of states. E.g. the peak with  $M = 8$  in Fig. 3 has  $\binom{26}{8} > 1.5 \cdot 10^6$  contributing states, about 5% of full Hilbert space containing  $2^{25}$  states. Nevertheless the NESS remain chiral, due to the cumulative chiral effect of all contributing components.

Finally, magnetization profile for all “phantom” manifolds  $0 < M \leq N/2$  remains qualitatively different from that of typical (non-chiral) NESS, see bottom panel of Fig. 4.

Due to larger number of contributing states, peaks with larger  $M$  are less sharp and have smaller amplitude, but, on the other side, the NESS gets more stable with respect to perturbations (boundary misfits, lowering dissipation, etc.). This effect can be seen by comparing the behavior of peaks at increasing  $\theta_R - \theta_L$  misfit (upper panel of Fig. 2) and for different  $\Gamma$  values (the bottom panel). In particular, as  $\Gamma$  decreases, the near Zeno limit description of an effectively coherent evolution (2) becomes invalid, and the peaks gradually smear out, the sharper peaks first.

In contrast, for parameters chosen away from “phantom” manifolds, variations of  $\Gamma$  do not lead to any drastic effects (data not shown), especially for large enough  $N$ . The reason is, beyond certain characteristic value  $\Gamma > \Gamma_{ch}(N) = O(1/N)$ , effective quantum Zeno regime sets in.

**Conclusion.** We demonstrated that the spikes of the steady magnetization current in open  $XXZ$  spin chains with dissipatively created boundary gradient are due to the existence of special manifolds (8) where phantom Bethe roots solutions of the Bethe Ansatz equations exist. The mechanism by which the chiral eigenstates emerging at the manifolds (8) can be physically accessed was identified to be the strong dissipation driving the system towards a chiral invariant subspace, gradually depopulat-

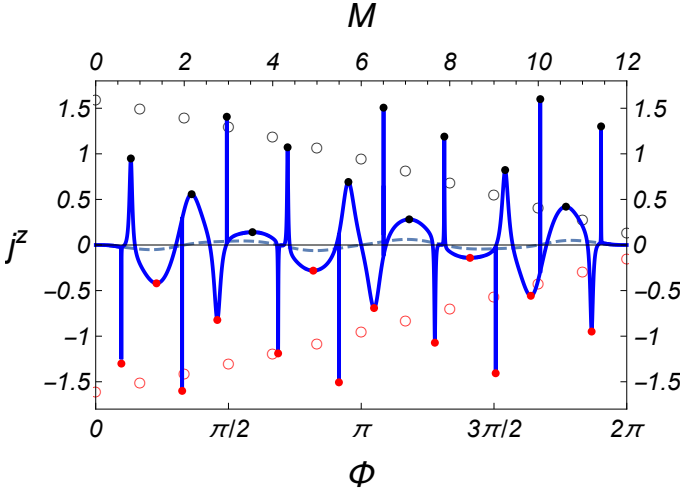


FIG. 3. Steady magnetization current  $j^z$  (blue curve) versus  $XY$ -plane misfit angle  $\Phi = \varphi_R - \varphi_L$  (bottom x-axis), in Zeno limit  $\Gamma \rightarrow \infty$ , computed using method in [30, 31]. Parameters are:  $N = 25$ ,  $\Delta = 0.6$ ,  $\theta = \pi/2$ .  $\Phi$  coordinates of black (red) circles correspond to angles  $\Phi_c(M) = \varphi_R - \varphi_L$  with  $M = 0, 1, \dots, N+1$  in (8). The dotted line close to the x axis shows  $j_z$  versus  $\Phi$  for a chain with an additional boundary misfit  $\pi/6$  in the polar angle:  $\vec{n}_L = (1, 0, 0)$ ,  $\vec{n}_R = (\frac{\sqrt{3}}{2} \cos \Phi, \frac{\sqrt{3}}{2} \sin \Phi, \frac{1}{2})$ . Inset (black and red empty circles) shows the dependence of  $j^z(\Phi_c(M))$  versus  $M$  (top x-axis), i.e. black and red points, ordered by their amplitude.

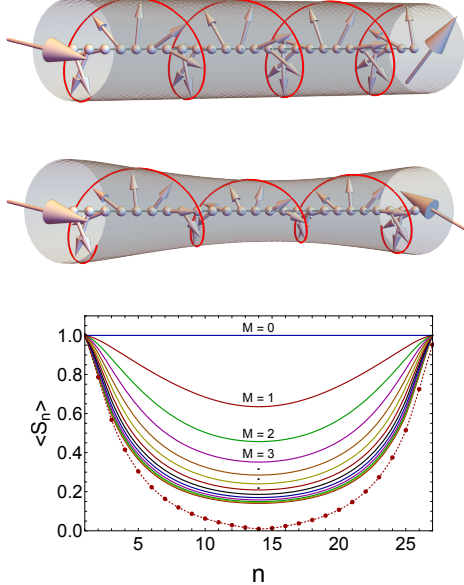


FIG. 4. **Top and middle panels.** PBS of the XXZ open chain with  $N = 25$  and for cases  $M = 0$  (top panel) and  $M = 1$  (middle panel) in Eq.(8). **Bottom panel:** Variation of the averaged spin (helix radius) along the chain for  $M = 0, 1, \dots, 12$  (curves from top to bottom, respectively). The dotted curve at the bottom, depicted for comparison, refers to a generic NESS out of the phantom manifold. All parameters are fixed as in Fig. 3.

ing the rest of the Hilbert space via a stochastic Markov process, similarly to the depopulation of the highly energetic states in a quantum system coupled to a cold thermal bath. The amplitude of dissipation plays the role of inverse temperature and a chiral subset of states plays the role of a subset of low-energy states close to the ground state of the system. By varying the system size, the bulk anisotropy and the boundary dissipative driving one can manipulate a number of peaks of the magnetization current, distance between the peaks in the parameter space, and their magnitudes. All the resulting stationary states are easily distinguishable by the value of the carried spin current, and nontrivial topology [32]. Simplest representatives of PBS, the spin-helix states, were recently obtained in experiments on cold atoms, where an XXZ chain with tunable anisotropy was implemented [33, 34].

VP acknowledges financial support from the European Research Council through the advanced grant No. 694544—OMNES, and from the Deutsche Forschungsgemeinschaft through the DFG project KL 645/20-1. VP thanks the Department of Physics "E.R.Caianiello" for hospitality and for short visits partial supports (FARB 2018 - 2019) during which the work was completed.

- 
- [1] F. Verstraete, M. M. Wolf, and J. I. Cirac, *NATURE PHYSICS* **5**, 633 (2009).
  - [2] P. Zanardi and L. C. Venuti, *PHYSICAL REVIEW LETTERS* **113** (2014), 10.1103/PhysRevLett.113.240406.
  - [3] V. V. Albert, B. Bradlyn, M. Fraas, and L. Jiang, *PHYSICAL REVIEW X* **6** (2016), 10.1103/PhysRevX.6.041031.
  - [4] S. Touzard, A. Grimm, Z. Leghtas, S. O. Mundhada, P. Reinhold, C. Axline, M. Reagor, K. Chou, J. Blumoff, K. M. Sliwa, S. Shankar, L. Frunzio, R. J. Schoelkopf, M. Mirrahimi, and M. H. Devoret, *PHYSICAL REVIEW X* **8** (2018), 10.1103/PhysRevX.8.021005.
  - [5] D. C. Cole, J. J. Wu, S. D. Erickson, P.-Y. Hou, A. C. Wilson, D. Leibfried, and F. Reiter, *NEW JOURNAL OF PHYSICS* **23** (2021), 10.1088/1367-2630/ac09c8.
  - [6] A. P. Orioli, J. K. Thompson, and A. M. Rey, *PHYSICAL REVIEW X* **12** (2022), 10.1103/PhysRevX.12.011054.
  - [7] G. Barontini, L. Hohmann, F. Haas, J. Esteve, and J. Reichel, *SCIENCE* **349**, 1317 (2015).
  - [8] T. Botzung, S. Diehl, and M. Müller, *Phys. Rev. B* **104**, 184422 (2021).
  - [9] C.-E. Bardyn, M. A. Baranov, C. V. Kraus, E. Rico, A. İmamoğlu, P. Zoller, and S. Diehl, *New Journal of Physics* **15**, 085001 (2013).
  - [10] C. Kollath, A. Sheikhan, S. Wolff, and F. Brennecke, *Phys. Rev. Lett.* **116**, 060401 (2016).
  - [11] J. T. Barreiro, M. Mueller, P. Schindler, D. Nigg, T. Monz, M. Chwalla, M. Hennrich, C. F. Roos, P. Zoller, and R. Blatt, *NATURE* **470**, 486 (2011).
  - [12] B. Kraus, H. P. Buechler, S. Diehl, A. Kantian, A. Micheli, and P. Zoller, *PHYSICAL REVIEW A* **78**



- (2008), [10.1103/PhysRevA.78.042307](#).
- [13] N. Yamamoto, *Phys. Rev. A* **72**, 024104 (2005).
- [14] V. Popkov and G. M. Schütz, *PHYSICAL REVIEW E* **95** (2017), [10.1103/PhysRevE.95.042128](#).
- [15] V. Popkov, X. Zhang, and A. Klümper, *Phys. Rev. B* **104**, L081410 (2021).
- [16] X. Zhang, A. Klümper, and V. Popkov, *Phys. Rev. B* **103**, 115435 (2021).
- [17] X. Zhang, A. Klümper, and V. Popkov, *Phys. Rev. B* **104**, 195409 (2021).
- [18] B. MISRA and E. SUDARSHAN, *JOURNAL OF MATHEMATICAL PHYSICS* **18**, 756 (1977).
- [19] K. Koshino and A. Shimizu, *PHYSICS REPORTS-REVIEW SECTION OF PHYSICS LETTERS* **412**, 191 (2005).
- [20] W. ITANO, D. HEINZEN, J. BOLLINGER, and D. WINELAND, *PHYSICAL REVIEW A* **41**, 2295 (1990).
- [21] P. Facchi, V. Gorini, G. Marmo, S. Pascazio, and E. Sudarshan, *PHYSICS LETTERS A* **275**, 12 (2000).
- [22] H. P. Breuer and F. Petruccione, *The theory of open quantum systems* (Oxford University Press, Great Clarendon Street, 2002).
- [23] See Supplemental Material.
- [24] H. SPOHN, *LETTERS IN MATHEMATICAL PHYSICS* **2**, 33 (1977).
- [25] V. Popkov, S. Essink, C. Presilla, and G. Schuetz, *PHYSICAL REVIEW A* **98** (2018), [10.1103/PhysRevA.98.052110](#).
- [26] Phantom Bethe roots criterium for open  $XXZ$  spin chain with boundary fields is given by Eq.(17) of [16]. For our special case  $h_D$  (1) we set  $\alpha_+ = \alpha_- = -\eta = -i\gamma$ ,  $\beta_+ + \beta_- = 0$ ,  $\theta_- = i(\pi - \varphi_L)$ ,  $\theta_+ = i(\pi - \varphi_R)$ ,  $1/\cosh(\beta_-) = \sin\theta_L$ ,  $\tanh(\beta_-) = -\cos\theta_L$ , leading to Eq.(8) with  $M = 0, \dots, N-1$ . Another choice of parameters  $\alpha_+ = \alpha_- = \eta = i\gamma$ ,  $\beta_+ + \beta_- = 0$ ,  $\theta_- = -i\varphi_L$ ,  $\theta_+ = -i\varphi_R$ ,  $1/\cosh(\beta_-) = \sin\theta_L$ ,  $\tanh(\beta_-) = \cos\theta_L$  leads to the same  $h_D$ . Inserting it into Eq.(17) of [16] leads to Eq.(8) with  $M \rightarrow M+2$ , thus enlarging the  $M$  range in (8) to values  $M = 0, \dots, N+1$ .
- [27] V. Popkov, S. Essink, C. Kollath, and C. Presilla, *Phys. Rev. A* **102**, 032205 (2020).
- [28] V. Popkov, C. Presilla, and J. Schmidt, *PHYSICAL REVIEW A* **95** (2017), [10.1103/PhysRevA.95.052131](#).
- [29] V. Popkov, J. Schmidt, and C. Presilla, *JOURNAL OF PHYSICS A-MATHEMATICAL AND THEORETICAL* **50** (2017), [10.1088/1751-8121/aa86cb](#).
- [30] V. Popkov, T. Prosen, and L. Zadnik, *PHYSICAL REVIEW LETTERS* **124** (2020), [10.1103/PhysRevLett.124.160403](#).
- [31] V. Popkov, X. Zhang, and T. Prosen, “Boundary driven XYZ chain: Exact inhomogeneous triangular matrix product ansatz,” [arXiv:arXiv:2112.05616 \[cond-mat.stat-mech\]](#).
- [32] T. Posske and M. Thorwart, *Phys. Rev. Lett.* **122**, 097204 (2019).
- [33] P. N. Jepsen, W. W. Ho, J. Amato-Grill, I. Dimitrova, E. Demler, and W. Ketterle, *Phys. Rev. X* **11**, 041054 (2021).
- [34] P. N. Jepsen, Y. K. Lee, H. Lin, I. Dimitrova, Y. Margalit, W. W. Ho, and W. Ketterle, “Catching Bethe phantoms and quantum many-body scars: Long-lived spin-helix states in Heisenberg magnets,” [arXiv:arXiv:2110.12043 \[cond-mat.quant-gas\]](#).
- [35] V. Popkov, T. Prosen, and L. Zadnik, *PHYSICAL REVIEW E* **101** (2020), [10.1103/PhysRevE.101.042122](#).

*Supplemental Material for*  
**Dissipative cooling towards phantom Bethe states  
in boundary driven XXZ spin chain**  
by Vladislav Popkov and Mario Salerno

**CONTENTS**

Acknowledgments	4
References	4
S-I. Lindblad Master equation and system evolution near Zeno limit	SM-1
S-II. Lindblad Master equation and its symmetries	SM-2
S-III. invariant subspace $W_M$ of $h_D$ at phantom Bethe manifolds	SM-3
S-IV. Properties of Markov process (3) at points $\Phi_c(M)$	SM-5

This Supplemental Material contains four sections. In [S-I](#) we collect some useful standard definitions. In [S-II](#) we derive symmetry properties of the Lindblad equation. In [S-III](#) we prove the existence of invariant subspaces at Bethe manifolds (8). In [S-IV](#) we analyze the effective Markov process (3).

**S-I. LINDBLAD MASTER EQUATION AND SYSTEM EVOLUTION NEAR ZENO LIMIT**

A density matrix of a quantum system with dissipation satisfies, under standard assumptions [18, 22], a Lindblad Master equation (LME),

$$\begin{aligned} \frac{\partial \rho(t)}{\partial t} &= -i[H_s, \rho] + \Gamma \mathcal{D}[\rho] \\ \mathcal{D}[\rho] &= \sum_{\gamma} \mathcal{D}_{L_{\gamma}}[\rho] = \sum_{\gamma} 2L_{\gamma}\rho L_{\gamma}^{\dagger} - (L_{\gamma}^{\dagger}L_{\gamma}\rho + \rho L_{\gamma}^{\dagger}L_{\gamma}), \end{aligned} \quad (\text{S1})$$

where  $H_s^{\dagger} = H_s$  is a coherent part,  $\mathcal{D}[\rho]$  is the dissipator, and  $L_{\gamma}$  are Lindblad operators, describing the interaction with the environment. Dissipative targeting of a pure qubit state  $|\psi\rangle\langle\psi|$  at single site is realized by dissipator  $\mathcal{D}_L[\rho]$  with  $L = |\psi\rangle\langle\psi^{\perp}|$ , where  $\langle\psi^{\perp}|\psi\rangle = 0$  and correspondingly  $\mathcal{D}_L[|\psi\rangle\langle\psi|] = 0$ . Normalization of states  $|\psi\rangle, |\psi^{\perp}\rangle$  entails  $\text{tr}(L^{\dagger}L) = 1$ .

The linear map  $\mathcal{D}_L[\rho]$  has 4 eigenmodes with eigenvalues  $0, -1, -1, -2$ . Therefore, a formal solution of (S1) with  $H_s \rightarrow 0$  and single operator  $L = |\psi\rangle\langle\psi^{\perp}|$  gives

$$\rho_1(t) = e^{-\Gamma \mathcal{D}_L t} \rho_1(0) = |\psi\rangle\langle\psi| + O(e^{-\Gamma t}) \quad (\text{S2})$$

at large times  $t$ . Approximately the same is true if  $\Gamma \gg \|H_s\|$ , so that coherent evolution can be considered as a perturbation.

In our setup Fig. 1 an open XXZ spin  $\frac{1}{2}$  chain consists of  $N + 2$  sites, numbered as  $0, 1, \dots, N + 1$ . We assume targeting of generic pure qubit states

$$\rho_{L,R} = \frac{1}{2} (I + \vec{n}_{L,R} \cdot \vec{\sigma}),$$

at sites 0 and  $N + 1$ , where  $\vec{n}_L, \vec{n}_R$  are unit vectors of polarization, parametrized in spherical coordinates by angles  $0 \leq \theta_L, \theta_R \leq \pi$  and  $0 \leq \varphi_L, \varphi_R < 2\pi$ . Explicitly,

$$\begin{aligned} \rho_{L,R} &= |\psi_{L,R}\rangle\langle\psi_{L,R}| \\ |\psi_Q\rangle^t &= \left( \cos \frac{\theta_Q}{2}, \quad e^{i\varphi_Q} \sin \frac{\theta_Q}{2} \right) \end{aligned}$$

The dissipator  $\mathcal{D}$  in (S1) thus has two Lindblad operators, acting at sites  $0, N+1$ ,

$$L_1 = |\psi_L\rangle\langle\psi_L^\perp| \otimes I^{\otimes N+1} \quad (\text{S3})$$

$$L_2 = I^{\otimes N+1} \otimes |\psi_R\rangle\langle\psi_R^\perp| \quad (\text{S4})$$

while the coherent part of the evolution is given by XXZ model with  $z$  anisotropy  $J_z/J_x = J_z/J_y = \Delta$ ,

$$H_s = g_0 \sum_{n=0}^N \sigma_n^x \sigma_{n+1}^x + \sigma_n^y \sigma_{n+1}^y + \Delta \sigma_n^z \sigma_{n+1}^z = g_0 \sum_{n=0}^N \vec{\sigma}_n \cdot \hat{J} \vec{\sigma}_{n+1}, \quad (\text{S5})$$

where  $\hat{J} = \text{diag}(1, 1, \Delta)$ . In the following and in the main text, we have chosen  $g_0 = 1$ .

It can be proved that the steady state of the (S1), i.e.

$$\lim_{t \rightarrow \infty} \rho(\Gamma, t) = \rho_{NESS}(\Gamma)$$

is unique for any given choice of targeted polarizations. In the Zeno limit we have

$$\lim_{\Gamma \rightarrow \infty} \rho_{NESS}(\Gamma) = \rho_{NESS}^{Zeno} = \rho_L \otimes R \otimes \rho_R \quad (\text{S6})$$

Remarkably, it was shown in [35] that Zeno NESS (S6) stays robust under possible asymmetry of dissipation between the left and the right boundary. Namely, rescaling of Lindblad operators  $L_1 \rightarrow \gamma L_1, L_2 \rightarrow L_2$  in (S1) with any finite nonzero  $\gamma$  yields the same limiting result (S6).

Now, it was shown in [25] that at time scale  $t = O(1)$  and large  $\Gamma$  the density matrix  $\rho(t)$  has approximate form (S6) with  $R$  substituted by  $R(t\Gamma) = R(\tau)$ , and the time evolution of  $R(\tau)$  is given by

$$\frac{\partial R(\tau)}{\partial \tau} = -i[h_D, R] + \frac{1}{\Gamma} \mathcal{D}_{eff}[R] \quad (\text{S7})$$

where  $\mathcal{D}_{eff}$  is an effective dissipator,  $h_D^\dagger = h_D$  is the so-called dissipation-projected Hamiltonian [2] has a form of a initial  $H_s$  restricted to the internal sites  $1, 2, \dots, N$ , with additional boundary fields, resulting from the dissipation [25]:

$$h_D = \sum_{n=1}^{N-1} \vec{\sigma}_n \cdot \hat{J} \vec{\sigma}_{n+1} + (\hat{J} \vec{n}_L) \cdot \vec{\sigma}_1 + (\hat{J} \vec{n}_R) \cdot \vec{\sigma}_N \quad (\text{S8})$$

It follows from (S6), (S7) that  $[h_D, R] = 0$  and that

$$R(\tau) = \sum_{\alpha} P_{\alpha}(\tau) |\alpha\rangle\langle\alpha| + O(\Gamma^{-1})$$

where  $|\alpha\rangle$  are  $h_D$  eigenvectors. Coefficients  $P_{\alpha}(\tau)$  evolve adiabatically, affected by perturbative effective dissipator  $\mathcal{D}_{eff}$  in (S7). This adiabatic evolution is given by Markov process with rates given in [25], properties of which are given in sec. S-IV.

## S-II. LINDBLAD MASTER EQUATION AND ITS SYMMETRIES

Let us define a unitary transformation describing a simultaneous rotation of all spins around  $z$  axis,

$$U_{\varphi} = \prod_{k=0}^{N+1} e^{i \frac{\varphi}{2} \sigma_k^z}$$

and the operator of the left-right reflection  $T_{Mirror}$ ,

$$T_{Mirror}(A \otimes B \otimes \dots \otimes C) T_{Mirror} = C \otimes \dots \otimes B \otimes A$$

Consider a Lindblad equation (S1) with targeted polarizations lying in  $XY$ -plane,  $\theta_L = \theta_R = \pi/2$ ,  $\varphi_L = 0$ , and arbitrary  $\varphi_R$ . Both  $T_{Mirror}$  and  $U(\varphi)$  leave the bulk Hamiltonian  $H_s$  (S5) invariant, while the Lindblad operators  $L_1, L_2$  from (S3), (S4) are transformed as

$$\begin{aligned} U_{\varphi_R} T_{Mirror} L_2 T_{Mirror} U_{\varphi_R}^\dagger &= L_1 \\ U_{\varphi_R} T_{Mirror} L_1 T_{Mirror} U_{\varphi_R}^\dagger &= e^{i\varphi_R \sigma_{N+1}^z} L_2 e^{-i\varphi_R \sigma_{N+1}^z} = L_2|_{\varphi_R \rightarrow -\varphi_R}, \end{aligned}$$

leading to the same physical setup with the opposite boundary gradient at the right boundary. Indeed, it is straightforward to verify that LME (S1) under transformation  $U_{\varphi_R} T_{Mirror} \dots T_{Mirror} U_{\varphi_R}^\dagger$  is mapped onto the same LME with opposite boundary gradient,  $\varphi_R \rightarrow -\varphi_R$ , the corresponding  $\rho$  being transformed into

$$\rho(-\varphi_R) = U_{\varphi_R} T_{Mirror} \rho(\varphi_R) T_{Mirror} U_{\varphi_R}^\dagger. \quad (\text{S9})$$

Uniqueness of the NESS for any choice of boundary parameters implies that the above transformation maps between NESS with opposite boundary gradients. In particular, for discrete set of  $\varphi_R$  values Eq.(8) in the main text parametrized by integer  $M_+$ ,  $\varphi_R(M_+) = (N+1-2M_+)\gamma$  we have  $\varphi_R(M_- \equiv N+1-M_+) = -\varphi_R(M_+)$ , and respectively, the transformation (S9) can be used to obtain NESS for  $M_-$  from the NESS for  $M_+$  as

$$\rho_{NESS}(\varphi_R(M_-)) = U_{\varphi_R(M_+)} T_{Mirror} \rho_{NESS}(\varphi_R(M_+)) T_{Mirror} U_{\varphi_R(M_+)}^\dagger. \quad (\text{S10})$$

Notably, the steady state current under the transformation  $\varphi_R \rightarrow -\varphi_R$  changes its sign,  $\langle j^z(M_-) \rangle = -\langle j^z(M_+) \rangle$ , which can be seen in Fig. 2 and Fig. 3 of the main text.

### S-III. INVARIANT SUBSPACE $W_M$ OF $h_D$ AT PHANTOM BETHE MANIFOLDS

Let us parametrize an arbitrary pure qubit state with two real parameters  $f, F$  as

$$|f, F\rangle = \frac{1}{\sqrt{1+e^{2f}}} \begin{pmatrix} 1 \\ e^{f+iF} \end{pmatrix}. \quad (\text{S11})$$

$$|F\rangle = \frac{1}{\sqrt{2}} \begin{pmatrix} 1 \\ e^{iF} \end{pmatrix} \quad (\text{S12})$$

State  $|f, F\rangle$  describes a spin 1/2 pointing in the direction  $(\langle \sigma^x \rangle, \langle \sigma^y \rangle, \langle \sigma^z \rangle) = (\sin \theta \cos F, \sin \theta \sin F, \cos \theta)$  with  $\tan(\theta/2) = e^f$ . Thus  $-\infty < f < \infty$  parametrizes a polar angle while  $0 \leq F < 2\pi$  is a azimuthal angle (or phase factor) in usual polar coordinates. State  $|F\rangle$  describes a fully polarized spin 1/2 lying in  $XY$ -plane. Here for simplicity we consider condition (8) at  $\theta = \pi/2$  (dissipation baths in  $XY$  plane).

We shall prove the following Theorem:

**Theorem.**— The set of states

$$|n_1, n_2, \dots, n_M\rangle = \bigotimes_{k=1}^{n_1-1} |k\varphi\rangle \bigotimes_{k=n_1}^{n_2-1} |(k-2)\varphi\rangle \dots \bigotimes_{k=n_M}^N |(k-2M)\varphi\rangle \quad (\text{S13})$$

$$1 \leq n_1 < n_2 < \dots < n_M \leq N+1 \quad (\text{S14})$$

form an invariant subspace  $W_M^+$  of  $h_D$  (S8) satisfying (8) with fixed  $M$  and  $\varphi_L = 0$ .

*Remark.*— In (S13)  $n_1 = 1$  and  $n_M = N+1$  denote virtual kinks at outer links of the chain  $(0, 1)$  and  $(N, N+1)$ :  $n_1 = 1$  and  $n_1 > 1$  correspond to first qubit in (S13) being  $|- \varphi\rangle$  and  $|\varphi\rangle$  respectively. Likewise,  $n_M = N+1$  and  $n_M < N+1$  correspond to the last qubit of the form  $|(N-2M+2)\varphi\rangle$  and  $|(N-2M)\varphi\rangle$  respectively.

Introduce notations

$$\begin{aligned} |F_1, F_2, \dots, F_m\rangle &= 2^{-m/2} \bigotimes_{k=1}^m \begin{pmatrix} 1 \\ e^{iF_k} \end{pmatrix} \\ F^\perp &= F + \pi; \quad |F^\perp\rangle = \sigma^z |F\rangle; \quad \langle F^\perp | F \rangle = 0 \end{aligned}$$



$\tilde{h}_D = h_D - (N-1)\Delta I$  can be written as sum of local terms

$$\tilde{h}_D = h_{12} + h_{23} + \dots + h_{N-1,N} + h_l \otimes I^{\otimes N-1} + I^{\otimes N-1} \otimes h_r \quad (\text{S15})$$

where

$$h = \sigma^x \otimes \sigma^x + \sigma^y \otimes \sigma^y + \Delta(\sigma^z \otimes \sigma^z - I \otimes I) \quad (\text{S16})$$

is the local energy -density of  $XXZ$  spin chain.

A key point in the proof is the divergence condition

$$h|F, F + \gamma\rangle = -\kappa|F^\perp, F + \gamma\rangle + \kappa|F, (F + \gamma)^\perp\rangle \quad (\text{S17})$$

$$\kappa = i \sin \gamma$$

$$\Delta = \cos \gamma \quad (\text{S18})$$

Using (S17) one obtains other useful relations:

$$(h_{12} + h_{23})|F, F + \gamma, F\rangle = -\kappa|F^\perp, F + \gamma, F\rangle - \kappa|F, F + \gamma, F^\perp\rangle + a_0|F, F + \gamma, F\rangle + a_+|F, F - \gamma, F\rangle \quad (\text{S19})$$

$$(h_{12} + h_{23})|F, F - \gamma, F\rangle = \kappa|F^\perp, F - \gamma, F\rangle + \kappa|F, F - \gamma, F^\perp\rangle + a_0|F, F - \gamma, F\rangle + a_-|F, F + \gamma, F\rangle \quad (\text{S20})$$

$$a_0 = -2\Delta; \quad a_\pm = 2e^{\pm i\gamma}. \quad (\text{S21})$$

Due to (S17), (S19), (S20), any factorized state of the form

$$\Psi = \otimes_{k=1}^N |0, F_k\rangle; \quad F_{k+1} - F_k = \pm\gamma \quad (\text{S22})$$

under action of  $\sum_{n=1}^{N-1} h_{n,n+1}$  will transform into sum of the terms of the same type (S22),  $\Psi_\alpha = \otimes_{k=1}^N |F_{k,\alpha}\rangle$ ;  $F_{k+1,\alpha} - F_{k,\alpha} = \pm\gamma$  plus two extra terms,

$$\begin{aligned} \sum_{n=1}^{N-1} h_{n,n+1} \Psi &= \sum_{\alpha} C_{\alpha} |F_1, F_{2,\alpha} F_{3,\alpha} \dots F_{N-1,\alpha}, F_N\rangle + A_1 |F_1^\perp, F_2, \dots, F_N\rangle + A_N |F_1, F_2, \dots, F_{N-1}, F_N^\perp\rangle \\ F_{2\alpha} - F_1 &= \pm\gamma, \quad F_{(k+1),\alpha} - F_{k,\alpha} = \pm\gamma; \quad F_N - F_{N-1,\alpha} = \pm\gamma \end{aligned}$$

where  $A_1 = \kappa \operatorname{sign}((F_1 - F_2)/\gamma)$ ,  $A_N = \kappa \operatorname{sign}((F_N - F_{N-1})/\gamma)$ .

All basis vector of  $W_M$  are of the form ((FF) with  $F_1 = \pm\gamma$ ,  $F_N = F_c(M) \pm \gamma$ . Acting by  $\tilde{h}_D$  on basis elements  $\|n_1 n_2 \dots n_M\rangle\rangle$  we generate other terms from the same basis  $\|m_1 m_2 \dots m_M\rangle\rangle \equiv |F_1, \dots, F_N\rangle$  and extra terms with "impurities" at site 1 and site  $N$ :

$$\begin{aligned} \tilde{h}_D \|n_1 n_2 \dots n_M\rangle\rangle &= \dots + A_1 |F_1^\perp, F_2, \dots\rangle + h_l \otimes I^{\otimes N-1} |F_1^\perp, F_2, \dots\rangle + \\ &+ A_N |\dots, F_{N-1}, F_N^\perp\rangle + (I^{\otimes N-1} \otimes h_r) |\dots, F_{N-1}, F_N^\perp\rangle \end{aligned}$$

Since  $A_1 = \operatorname{sign}((F_1 - F_2)/\gamma)\kappa$ ,  $F_1 = \pm\gamma$ , four terms  $A_1 |F_1^\perp, F_2 \dots\rangle$  may arise:

$$A_1 |F_1^\perp, F_2, \dots\rangle = \kappa |-\gamma^\perp, -2\gamma, \dots\rangle, \quad -\kappa |\gamma^\perp, 2\gamma, \dots\rangle \quad (\text{S23})$$

$$A_1 |F_1^\perp, F_2, \dots\rangle = \kappa |\gamma^\perp, 0, \dots\rangle, \quad -\kappa |-\gamma^\perp, 0, \dots\rangle \quad (\text{S24})$$

Terms of type (S23) are cancelled with respective  $h_l \otimes I^{\otimes N-1} |F_1, F_2 \dots\rangle$ , using relations

$$h_l |\pm\gamma\rangle = \pm\kappa |\pm\gamma^\perp\rangle + \Delta |\pm\gamma\rangle \quad (\text{S25})$$

For terms of type (S24) one uses another relation:

$$h_l |\pm\gamma\rangle = \mp\kappa |\pm\gamma^\perp\rangle - \Delta |\pm\gamma\rangle + 2e^{\pm i\gamma} |\mp\gamma\rangle \quad (\text{S26})$$

Likewise, four terms of type  $A_N|\dots F_{N-1}, F_N^\perp\rangle$  can arise: denoting

$$\Phi_c(M) = (N + 1 - 2M)\gamma, \quad (\text{S27})$$

we obtain

$$A_N|\dots F_{N-1}, F_N^\perp\rangle = -\kappa|\dots, \Phi_c + 2\gamma, (\Phi_c + \gamma)^\perp\rangle, \quad \kappa|\dots, \Phi_c - 2\gamma, (\Phi_c - \gamma)^\perp\rangle, \quad (\text{S28})$$

$$A_N|\dots F_{N-1}, F_N^\perp\rangle = \kappa|\dots, \Phi_c, (\Phi_c + \gamma)^\perp\rangle, \quad -\kappa|\dots, \Phi_c, (\Phi_c - \gamma)^\perp\rangle, \quad (\text{S29})$$

Terms (S28),(S29) cancel with respective terms  $I^{\otimes N-1} \otimes h_r|\dots F_{N-1}, F_N\rangle$  using

$$h_r|\Phi_c \pm \gamma\rangle = \pm\kappa|(\Phi_c \pm \gamma)^\perp\rangle + \Delta|\Phi_c \pm \gamma\rangle \quad (\text{S30})$$

$$h_r|\Phi_c \pm \gamma\rangle = \mp\kappa|(\Phi_c \pm \gamma)^\perp\rangle - \Delta|\Phi_c \pm \gamma\rangle + 2e^{\pm i\gamma}|\Phi_c \mp \gamma\rangle, \quad (\text{S31})$$

respectively. Note that Eqs (S30), (S31) can be obtained from (S25), (S26) by rotation by angle  $\Phi_c(M)$ . In this way we deduce that action of  $h_D$  on any basis vector of  $W_M$  belongs to  $W_M$ , thus proving the Theorem (QED).

In addition, we find that the repeated action of  $h_D$  on any single basis vector generates the whole subspace  $W_M$ . It follows that all eigenvectors  $|\alpha_+\rangle \in W_M$  of  $h_D$  have nonzero overlaps with all vectors  $||n_1 \dots n_M\rangle\rangle$  of  $W_M$  basis. The total number of states in  $W_M$  in (S13) can be easily calculated on combinatorial grounds as

$$\dim W(M) = \binom{N+1}{M} = \binom{N}{M} + \binom{N}{M-1}$$

**Remark 1.**– The subspace  $W_M$  is a part of a larger invariant subspace  $G_M^+$  described in [16].  $G_M^+$  contains all vectors of  $W_M$  plus additional linearly independent vectors, all with qualitatively the same chirality features. The total number of vectors in  $G_M^+$  is

$$\dim G_M^+ = \binom{N}{M} + \binom{N}{M-1} + \binom{N}{M-2} + \dots + \binom{N}{0},$$

see [16]. Appearance of smaller invariant subspace  $W(M)$  within  $G_M^+$  is a consequence of a special form of the boundary fields in the dissipation-projected Hamiltonian (S8).

#### S-IV. PROPERTIES OF MARKOV PROCESS (3) AT POINTS $\Phi_c(M)$

The effective Markov evolution

$$\frac{\partial P_\alpha(\tau)}{\partial \tau} = \sum_{\beta \neq \alpha} w_{\beta\alpha} P_\beta(\tau) - \sum_{\beta \neq \alpha} w_{\alpha\beta} P_\alpha(\tau) \quad (\text{S32})$$

for the probabilities  $P_\alpha$  of occupation of state  $\alpha$  at time  $\tau$  is related to a reduced density matrix dynamics  $R(\tau)$  near quantum Zeno limit by

$$R(\tau) \approx \sum_{\alpha=1}^{\dim \mathcal{H}} P_\alpha(\tau) |\alpha\rangle \langle \alpha|$$

where  $\dim \mathcal{H} = 2^N$  is dimension of Hilbert space, and  $|\alpha\rangle$  are eigenvectors of  $h_D$ .

The rates  $w_{\alpha\beta} \equiv w_{\alpha \rightarrow \beta}$  are given by [25]

$$w_{\alpha\beta} = |\langle \beta | g_L | \alpha \rangle|^2 + |\langle \beta | g_R | \alpha \rangle|^2 \quad (\text{S33})$$

with some locally acting operators  $g_L, g_R$  [25].

On phantom Bethe manifolds parametrized by integer number  $M$ , existence of invariant subspaces of  $h_D$ :  $G_M^+, G_M^-$  and  $W_M \in G_M^+$  allows to split the  $h_D$  eigenvectors  $|\alpha\rangle$  into three blocks, as

$$\begin{aligned}
R(t) \approx & \sum_{\alpha_+=1}^{\dim(W_M)} P(\alpha_+, t) |\alpha_+\rangle \langle \alpha_+| + \sum_{\beta_+=\dim(W_M)+1}^{\dim(G_M^+)} P(\beta_+, t) |\beta_+\rangle \langle \beta_+| \\
& + \sum_{\gamma_-=1}^{\dim(G_M^-)} P(\gamma_-, t) |\gamma_-\rangle \langle \gamma_-|.
\end{aligned} \tag{S34}$$

corresponding to respective  $h_D$  eigenvalues  $\{\lambda_{\alpha_+}\}$ ,  $\{\lambda_{\beta_+}\}$  and  $\{\lambda_{\gamma_-}\}$ . In the Eq (S34), the first two block contributions share the same chirality (indicated with " + " subscript).

It was proved in [16] that states in  $G_M^+$ ,  $G_M^-$  are mutually orthogonal. If the sets  $\{\lambda_{\alpha_+}\}$ ,  $\{\lambda_{\beta_+}\}$  have no intersection,

$$\{\lambda_{\alpha_+}\} \cap \{\lambda_{\beta_+}\} = \emptyset. \tag{S35}$$

then also states  $|\alpha_+\rangle$ ,  $|\beta_+\rangle$  are also orthogonal.

We will be interested in cumulative probability current towards set of states in  $W_M$  from other blocks, given by

$$J_{\beta_+, \gamma_- \rightarrow \alpha_+}(t) = \sum_{\alpha: |\alpha\rangle \in W_M} \sum_{\gamma: |\gamma\rangle \notin W_M} (P(\gamma, t) w_{\gamma\alpha} - P(\alpha, t) w_{\alpha\gamma}) \tag{S36}$$

First, we notice that all basis vectors  $\|n_1, n_2, \dots, n_M\rangle\rangle$  of  $W_M$  eigenvectors of operators  $g_L, g_R$  in (S33):

$$\begin{aligned}
g_L \|n_1, n_2, \dots, n_M\rangle\rangle &= (2\delta_{n_1, 1} - 1) i \sin \varphi \|n_1, n_2, \dots, n_M\rangle\rangle \\
g_R \|n_1, n_2, \dots, n_M\rangle\rangle &= (1 - 2\delta_{n_M, N+1}) i \sin \varphi \|n_1, n_2, \dots, n_M\rangle\rangle,
\end{aligned}$$

entailing all

$$w_{\alpha\gamma} = 0; \quad |\alpha\rangle \in W_M, \quad |\gamma\rangle \notin W_M, \tag{S37}$$

provided (S35). On the other hand, at least some of  $w_{\gamma\alpha}$  rates in (S36) are strictly positive, since  $W_M$  basis states  $\langle\langle n_1 n_2 \dots n_M \|$  are not left eigenvectors of  $g_L, g_R$ . Consequently,

$$w_{\gamma\alpha} > 0; \quad |\alpha\rangle \in W_M, \quad |\gamma\rangle \notin W_M, \text{ for some } \gamma. \tag{S38}$$

Eqs(S37), (S38) show that one has strictly positive probability current (S36) at all times, leading to cumulative monotonous depopulation of states  $\sum_{\beta_{\pm}} P(\beta_{\pm}, t) \rightarrow 0$  and gradual increase of cumulative population of states  $\sum P(\gamma, t) \rightarrow 0$  with time. In the long time limit, only contributions from the invariant subspace  $W_M$  in (S34) remain, leading to

$$R(t \rightarrow \infty) = \sum_{\alpha_+=1}^{\dim(W_M)} P(\alpha_+, t) |\alpha_+\rangle \langle \alpha_+| + O(\Gamma^{-1})$$